Prognostic value of T-cell density in the tumor center and outer margins in gastric cancer

Soeratram, T.T.D.; Biesma, H.D.; Egthuijsen, J.M.P.; Kranenbarg, E.M.K.; Hartgrink, H.H.; Velde, C.J.H. van de; ... ; Grieken, N.C.T. van

Mod Pathol 36 (2023) 100218

MODERN PATHOLOGY

USCAP UNITED STATES AND CANADIAN ACADEMY OF PATHOLOGY
Creating a Better Pathologist

Journal homepage: https://modernpathology.org/

Research Article

Prognostic Value of T-Cell Density in the Tumor Center and Outer Margins in Gastric Cancer

Tanya T.D. Soeratram[a,b], Hedde D. Biesma[a,b], Jacqueline M.P. Egthuijsen[a,b], Elma Meershoek-Klein Kranenbarg[c], Henk H. Hartgrink[c], Cornelis J.H. van de Velde[c], Aart Mookhoek[d], Erik van Dijk[a,b], Yongsoo Kim[a,b], Bauke Ylstra[a,b], Hanneke W.M. van Laarhoven[b,e], Nicole C.T. van Grieken[a,b,*]

[a] *Department of Pathology, Amsterdam UMC location Vrije Universiteit Amsterdam, Amsterdam, The Netherlands;* [b] *Cancer Center Amsterdam, Cancer Biology and Immunology, Amsterdam, The Netherlands;* [c] *Department of Surgery, Leiden University Medical Center, Leiden, The Netherlands;* [d] *Department of Pathology, University of Bern, Bern, Switzerland;* [e] *Department of Medical Oncology, Amsterdam UMC location University of Amsterdam, Amsterdam, The Netherlands*

ARTICLE INFO

Article history:
Received 27 January 2023
Revised 28 March 2023
Accepted 8 May 2023
Available online 12 May 2023

Keywords:
CD8-positive T cells
FOXP3
gastric cancer
invasive margin
prognostic marker
regulatory T cells
tumor-infiltrating lymphocytes

ABSTRACT

Tumor-infiltrating lymphocytes are associated with the survival of gastric cancer patients. T-cell densities in the tumor and its periphery were previously identified as prognostic T-cell markers for resectable gastric cancer. Immunohistochemistry for 5 T-cell markers, CD3, CD45RO, CD8, FOXP3, and granzyme B was performed on serial sections of N = 251 surgical resection specimens of patients treated with surgery only in the D1/D2 trial. Positive T cells were digitally quantified into tiles of 0.25 mm^2 across 3 regions: the tumor center (TC), the inner invasive margin, and the outer invasive margin (OIM). A classification and regression tree model was employed to identify the optimal combination of median T-cell densities per region with cancer-specific survival (CSS) as the outcome. All statistical tests were 2-sided. $CD8_{OIM}$ was identified as the most dominant prognostic factor, followed by $FOXP3_{TC}$, resulting in a decision tree containing 3 prognostically distinct subgroups with high (Hi) or low (Lo) density of the markers: $CD8_{OIM}^{Hi}$, $CD8_{OIM}^{Lo}/FOXP3_{TC}^{Hi}$, and $CD8_{OIM}^{Lo}/FOXP3_{TC}^{Lo}$. In a multivariable Cox regression analysis, which included pathological T and N stages, Lauren histologic types, EBV status, microsatellite instability, and type of surgery, the immune subgroups were independent predictors for CSS. CSS was lower for $CD8_{OIM}^{Lo}/FOXP3_{TC}^{Hi}$ (HR: 5.02; 95% CI: 2.03-12.42) and for $CD8_{OIM}^{Lo}/FOXP3_{TC}^{Lo}$ (HR: 7.99; 95% CI: 3.22-19.86), compared with $CD8_{OIM}^{Hi}$ ($P < .0001$). The location and density of both $CD8^+$ and $FOXP3^+$ T cells in resectable gastric cancer are independently associated with survival. The combination of $CD8_{OIM}$ and $FOXP3_{TC}$ T-cell densities is a promising stratification factor that should be validated in independent studies.

Introduction

Gastric cancer (GC) is one of the most common causes of cancer-related death.[1] Despite the advances that have been made, 5-year survival rates of resectable GC remain around 40%.[2] This may partially be explained by the microenvironmental,

* Corresponding author.
E-mail address: nct.vangrieken@amsterdamumc.nl (N.C.T. van Grieken).

https://doi.org/10.1016/j.modpat.2023.100218

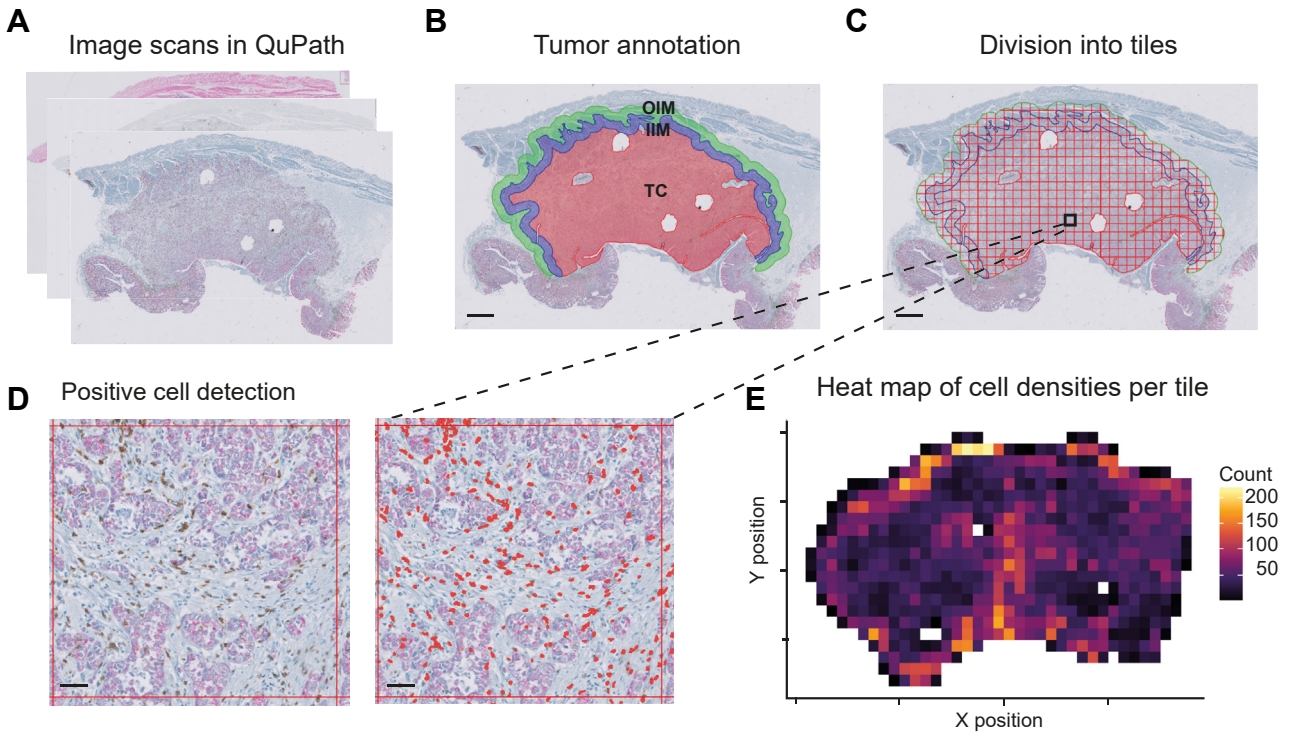

Figure 1.
Digital image analysis workflow. (A) Digital image scans of immunohistochemical stainings of the same tumor. (B) $CD8^+$PanCK staining with annotated tumor tissue and division into 3 regions: tumor center (TC), inner invasive margin (IIM), and outer invasive margin (OIM). (C) The annotated regions are divided into 0.5 mm^2 tiles. (D) $CD8^+$ cells detected by QuPath in a tile from the TC. (E) Cell counts and density were calculated for each 0.5 mm^2 tile. Scale bars annotate 1 mm (B, C) or 50 μm (D).

morphologic, and molecular characteristics of GC.[3] Based on these characteristics, various classifications[4,5] have been made to uncover distinct subgroups that may stratify patients for specific treatments.[6]

T cells are frequently studied as prognostic biomarkers because of their central role in the adaptive antitumor response and inhibition of tumor progression.[7] Cytotoxic $CD8^+$ T cells are particularly important because of their tumor-killing capacity with cytotoxic molecules such as granzyme B (GrzB). However, evolving tumors develop mechanisms to evade the cytotoxic T cells and escape their immune-mediated destruction.[8] Examples of such mechanisms are the recruitment of the immune suppressive $FOXP3^+$ regulatory T cells (Tregs)[9] or the upregulation of immune checkpoints,[7] which have an adverse effect on prognosis.

High numbers of T cells in the tumor microenvironment have been associated with improved survival in various cancers, including GC.[10] For GC, high numbers of $CD3^+$ and $CD8^+$ T cells were associated with improved prognosis in 2 meta-analyses.[11,12] However, contradictory results have been published on the prognostic value of the regulatory $FOXP3^+$ Tregs because associations with poor and improved survival have been reported.[11,12] Studies on $CD45RO^+$ memory T cells and the cytotoxic enzyme GrzB are limited in GC, yet indicative of a positive prognostic value[12-14] also shown for colorectal cancer.[15]

Differences in the reported prognostic value of the T-cell markers may be explained in part by the heterogeneity of the tumor immune microenvironment. In various published studies[13,14,16-19], small tissue regions or tissue microarrays were analyzed, impeding consideration of intratumoral heterogeneity.

In this study, we analyzed T-cell densities in the tumor microenvironment for their prognostic value. Because we analyzed tumor materials of patients with GC treated with surgery only, T-cell densities may also reflect tumor biology. To capture intratumoral heterogeneity, we performed a comprehensive digital image analysis of the tumor area using whole-section images of surgical resection specimens. The T-cell markers CD3 (general), CD45RO (memory), CD8 (cytotoxic), FOXP3 (regulatory), and cytotoxic enzyme GrzB were included because of their reported prognostic value in GC.[12]

Materials and Methods

Patients and Samples

Formalin-fixed and paraffin-embedded surgical resection material was used from patients with nonintramucosal gastric adenocarcinoma who participated in the Dutch D1/D2 trial.[20] In this trial, 1078 patients underwent randomly assigned resection with D1 or D2 lymph node dissection and 711 with curative intent. None of the patients received (neo)adjuvant chemo- or radiotherapy. The tumor stage was updated according to the eighth edition of the American Joint Committee on Cancer TNM classification.[21] Histologic tumor type was determined according to the Lauren classification as described previously.[22,23] The study was conducted in accordance with the Declaration of Helsinki and the Dutch Code of Conduct for Health Research.[24]

Immunohistochemistry

Immunohistochemistry (IHC) was performed on consecutive sections for CD3, CD45RO, FOXP3, GrzB, and a duplex IHC for CD8 and the epithelial marker pan-cytokeratin. All stainings were

automated with the Ventana Benchmark Ultra Slide Stainer (Roche Diagnostics) (Supplementary Methods).

Digital Image Analysis

Stainings were digitized with the IntelliSite Ultra Fast scanner (Philips) at a 40 x magnification (0.25 μm/pixel). The images were analyzed with QuPath software version 2.3.0[25] (Fig. 1). The tumor border was manually annotated in each staining. The invasive margin (IM) was automatically annotated by the expansion of an arbitrary width of 0.5 mm toward the inside and the outside of the tumor border, creating an inner invasive margin (IIM) and an outer invasive margin (OIM).[26] The remaining tumor area was defined as the tumor center (TC). Normal mucosa, necrosis, and artifacts were manually excluded from the analysis. Positive cell detection was performed separately for the 3 regions (TC, IIM, IOM) using a grid with 0.25 mm^2 tiles. The settings and threshold for positive cell detection were optimized for each of the 5 markers and were applied to all sections (Supplementary Table S1). Densities were calculated in cells/mm^2 per tile. The median density of all tiles per tumor was used for downstream analysis. In addition, intraepithelial and stromal $CD8^+$ T cells were assessed in the CD8/pan-cytokeratin duplex IHC (Supplementary Methods).

Assessment of The Cancer Genome Atlas Molecular Subgroups

Molecular subgroups were determined as described by The Cancer Genome Atlas (TCGA).[4] Epstein-Barr virus-positive (EBV^+) and microsatellite instability (MSI)-high tumors were identified previously for these samples.[22] Shallow whole genome sequencing was performed for the EBV-negative (EBV^-) and microsatellite stable tumors to retrieve copy number profiles,[22] which were used to classify the tumors into the genomically stable (GS) or chromosomal instable (CIN) subgroups as described for these samples (H.D. Biesma, T.T.D. Soeratram, H.F. van Essen, J.M.P. Egthuijsen, J.B. Poell, E. van Dijk *et al.* Copy number-based molecular subgroups and Lauren's histological subgroup are independent biological characteristics that determine survival in patients with resectable GC treated with surgery only, manuscript submitted).

Statistical Analysis

Immune cell densities were compared between the 3 regions using Kruskall-Wallis and pairwise Wilcoxon rank sum tests. Correlation coefficients between all immune markers in the 3 regions and their statistical significance were assessed using Spearman's rank test. Cancer-specific survival (CSS) time was calculated from the moment of surgery until the progression or recurrence of disease or GC-related death. Survival differences were analyzed by Kaplan-Meier and the log-rank test. Classification and regression tree (CART) analysis was performed to construct a decision tree. The most prognostic immune markers and the optimal cut-off values for high and low immune cell densities were determined. CSS was used as a dependent outcome variable in the CART model, with all numeric cell density markers in TC and OIM as independent predicting variables. The performance of the CART model and validity of the selected prognostic markers were assessed with 5-fold cross-validation and Lasso Cox regression analysis (Supplementary Methods). Multivariable Cox proportional hazard regression was performed to assess the association with survival while controlling for other prognostic variables. Statistical analyses were performed using R-Studio version 4.0.3. (Supplementary Methods).

Table 1
Baseline characteristics of 251 patients

Patient characteristics	N (%)
Sex	
Male	142 (56.6)
Female	109 (43.4)
Age (y)	
≤70	179 (71.3)
>70	72 (28.7)
Surgery	
D1	130 (51.8)
D2	121 (48.2)
Died within 30 d after surgery	
No	238 (94.8)
Yes	13 (5.2)
Tumor location	
Proximal	26 (10.4)
Middle	62 (24.7)
Distal	127 (50.6)
Whole stomach	36 (14.3)
Resection margin	
R0	217 (86.5)
R1	34 (13.5)
pT stage	
T1a	2 (0.8)
T1b	29 (11.6)
T2	35 (13.9)
T3	98 (39.0)
T4a	80 (31.9)
T4b	7 (2.8)
pN stage	
N0	84 (33.5)
N1	46 (18.3)
N2	53 (21.1)
N3a	50 (19.9)
N3b	18 (7.2)
M stage	
M0	240 (95.6)
M1	11 (4.4)
Stage (TNM eighth edition)	
Stage IA	24 (9.6)
Stage IB	20 (8.0)
Stage IIA	41 (16.3)
Stage IIB	35 (13.9)
Stage IIIA	60 (23.9)
Stage IIIB	42 (16.7)
Stage IIIC	18 (7.2)
Stage IV	11 (4.4)
Lauren	
Diffuse	79 (31.5)
Intestinal	115 (45.8)
Mixed	23 (9.2)
Other	34 (13.5)
EBV status	
EBV^-	228 (90.8)
EBV^+	23 (9.2)
MSI status	
MSS	229 (91.2)
MSI-high	22 (8.8)

EBV, Epstein-Barr virus; MSI, microsatellite instable; MSS, microsatellite stable; pN, pathological N stage; pT, pathological T stage; TNM, Tumor Regional Lymph Node and Metastasis Classification of Malignant Tumors according to eighth edition.

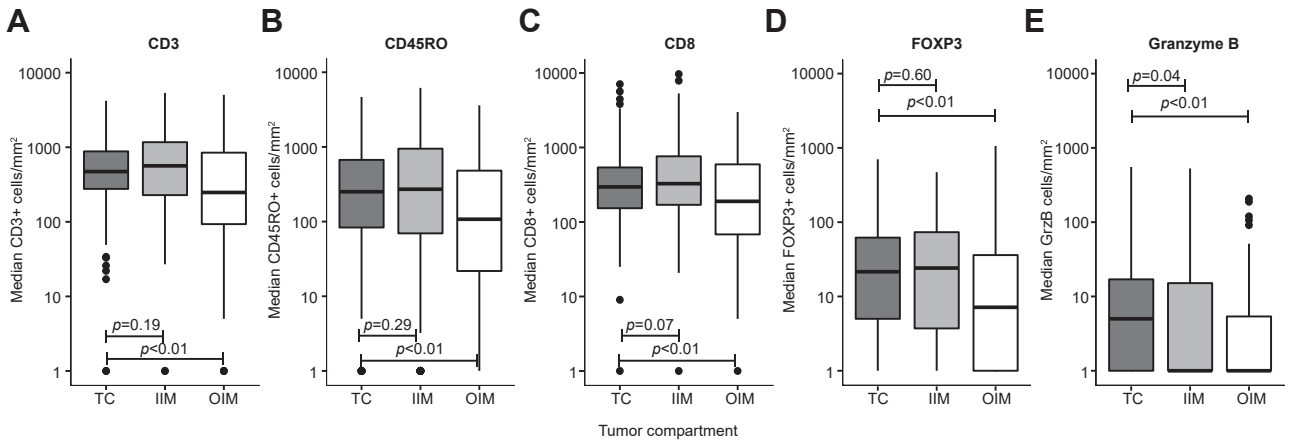

Figure 2.
The median immune cell densities in the tumor center (TC), inner invasive margin (IIM), and outer invasive margin (OIM). The median cell density (cells/mm^2) of (A) CD3, (B) CD45RO, (C) CD8, (D) FOXP3, and (E) granzyme B (GrzB) within the TC, IIM, and OIM of all patients. The boxplots depict median density and IQR (25% to 75%). The Wilcoxon rank sum test was used to calculate *P* values. To depict the densities on the log10 y-axis, density was offset by 1. Statistics were performed before log transformation.

Results

We collected tumor blocks of surgical resection specimens from 251 patients with resectable cancer (Supplementary Fig. S1). Patient characteristics are depicted in Table 1 and were comparable to the original trial cohort,[20] except for tumor stage due to the exclusion of intramucosal GC.

Immune Cell Densities in the Tumor Center, Inner Invasive Margin, and Outer Invasive Margin

The T-cell density of all markers showed considerable heterogeneity within 1 tumor section and between tumors (Supplementary Fig. S2). The median density (IQR) was 471 (604) for CD3$^+$, 250 (587) for CD45RO$^+$, 295 (387) for CD8$^+$, 21 (57) for FOXP3$^+$, and 4 (16) for GrzB$^+$ cells/mm^2 in the TC. T-cell densities were significantly higher in the TC compared with the OIM (Fig. 2, $P < .001$, Wilcoxon rank sum test) but not compared with the IIM. The IIM was highly correlated with the TC (Spearman correlation $R > 0.8$, $P < .05$, Supplementary Fig. S3) and therefore was excluded from further analyses.

Tumors with Lauren's intestinal type showed increased T-cell densities, mainly in the OIM, compared with the diffuse type ($P < .01$, Wilcoxon rank sum test, Supplementary Fig. S4). Mixed-type tumors showed immune densities comparable to diffuse-type tumors.

Significantly higher CD3, CD8, CD45RO, and GrzB densities in the TC and OIM were detected in the EBV$^+$ and MSI-high TCGA molecular subgroups than in the GS and CIN subgroups ($P < .05$, Wilcoxon rank sum test, Supplementary Fig. S5). Still, no difference in FOXP3 density was detected among the TCGA molecular subgroups.[4] No significant differences in any of the T-cell markers were found between the GS and CIN subgroups.

Association of Immune Cell Densities With Survival

To detect associations of immune cell marker densities with survival, the densities per marker and region were categorized into 4 groups, each with an equal number of tumors (Q1 to Q4). Kaplan-Meier plots of each marker in the TC and OIM for CSS are provided in Supplementary Figure S6. Patients with the highest T-cell densities (Q4) showed a favorable survival, which was significant for CD3, CD45RO, CD8, and FOXP3 (TC and OIM, $P < .05$, log-rank test). Higher T-cell densities were also associated with a lower pathological T stage for $CD8_{OIM}$, $FOXP3_{TC}$, and $FOXP3_{OIM}$ and a lower pathological N stage for all markers (linear trend test $P < .05$, Supplementary Fig. S7).

Selecting the Most Prognostic Markers Using Classification and Regression Tree Analysis

We used CART analysis that combined the most significant prognostic markers to determine an optimal cut-off value for maximal survival difference. The most significant prognostic marker in the decision tree was $CD8_{OIM}$, with a cut-off value of 798 CD8$^+$ T cells/mm^2 (Fig. 3A). The second marker in the decision tree was $FOXP3_{TC}$, with a cut-off value of 20 cells/mm^2. No other markers were selected by the CART analysis, resulting in a final tree with 3 subgroups: $CD8_{OIM}{}^{Hi}$ (Fig. 3B), $CD8_{OIM}{}^{Lo}/FOXP3_{TC}{}^{Hi}$ (Fig. 3C), and $CD8_{OIM}{}^{Lo}/FOXP3_{TC}{}^{Lo}$ (Fig. 3D), with a 10-year CSS of 80%, 48%, and 15%, respectively ($P < .001$, log-rank test, Fig. 3E).

A 5-fold cross-validation (80% of samples for training and 20% for testing) was performed to assess the robustness of model performance and the selected prognostic markers. The Cox regression likelihood ratio test was significant in 4 of 5 cross-validation folds (Supplementary Table S2). In particular, $FOXP3_{TC}$ was selected in all significant models and $CD8_{OIM}$ in 3 out of 4 significant models. In an alternative Lasso Cox regression model, both $CD8_{OIM}$ and $FOXP3_{TC}$ were selected as the most important prognostic markers (Supplementary Fig. S8), further indicating the robustness of the prognostic markers obtained with CART.

Clinical Parameters and T-Cell Densities in the Immune Subgroups

We further investigated the characteristics of immune subgroups identified by CART, including their association with known prognostic factors. The $CD8_{OIM}{}^{Hi}$ subgroup was enriched in EBV$^+$ (38.4%) and MSI-high (17.6%) tumors, intestinal type tumors (61%), and lower N stages (pN1/2 58%) (Fig. 3F). Also, in the Kaplan-Meier analysis of the TCGA molecular subgroups separately, the $CD8_{OIM}{}^{Hi}$ immune subgroup had the most favorable outcome in the EBV, GS, and CIN subgroups (Supplementary Fig. S9).

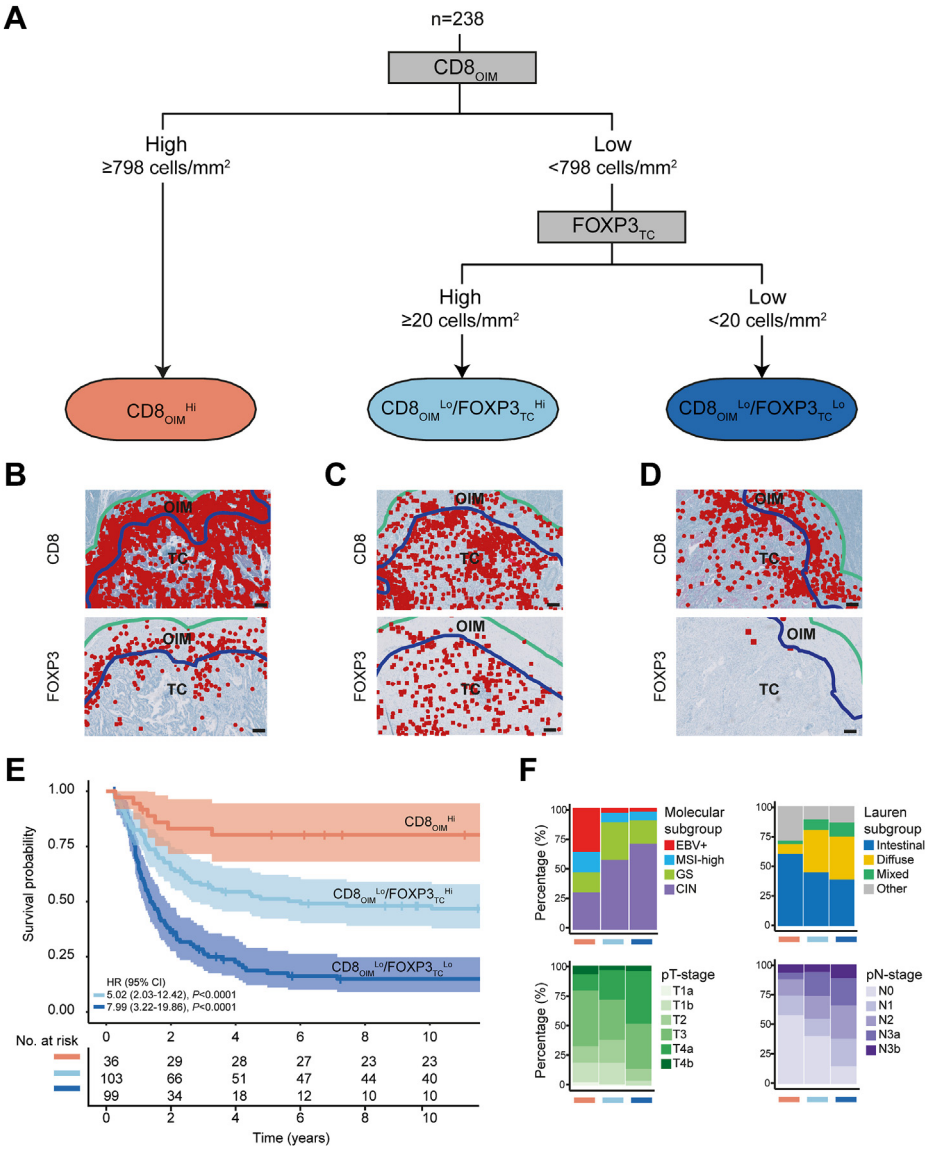

Figure 3.
Classification and regression tree (CART) analysis and association with histopathological variables. (A) Resulting tree from CART analysis of 238 patients with CD8 in the outer invasive margin (OIM) and FOXP3 in the tumor center (TC) as splitting variables and cancer-specific survival as an outcome. (B-D) Representative images of digitally quantified $CD8^+$ and $FOXP3^+$ cells of tumors from different CART subgroups: (B) $CD8_{OIM}{}^{Hi}$, (C) $CD8_{OIM}{}^{Lo}/FOXP3_{TC}{}^{Hi}$, and (D) $CD8_{OIM}{}^{Lo}/FOXP3_{TC}{}^{Lo}$. (E) Kaplan-Meier analysis of cancer-specific survival with CART subgroups as a factor. Multivariate Cox regression was used to calculate significant survival differences. (F) The distribution of TCGA molecular subgroups, Lauren histologic types, pT stage, and pN stage across the CART subgroups. CIN, chromosomal unstable; EBV, Epstein-Barr virus; GS, genomically stable; Hi, high; HR, hazard ratio; Lo, low; MSI, microsatellite instability; TCGA, The Cancer Genome Atlas.

In the $CD8_{OIM}{}^{Hi}$ subgroup, the density of $CD8_{TC}$, $CD3_{TC+OIM}$, $CD45RO_{TC+OIM,}$ and $GrzB_{TC+OIM}$ was also significantly higher than that in the $CD8_{OIM}{}^{Lo}$ subgroups (Fig. 4A-E). $FOXP3_{TC}$ density did not significantly differ between the $CD8_{OIM}{}^{Hi}$ and the $CD8_{OIM}{}^{Lo}/FOXP3_{TC}{}^{Hi}$ subgroups. However, the $FOXP3_{TC}/CD8_{TC}$ ratio was significantly lower in the $CD8_{OIM}{}^{Hi}$ subgroup (Fig. 4F).

To determine the cytotoxic activity of $CD8^+$ cells, the $GrzB_{TC}/CD8_{TC}$ and the intraepithelial/stromal $CD8_{TC}$ ratio were calculated. In relation to the total density of $CD8^+$ cells, more intraepithelial $CD8^+$ cells (Fig. 4G) and more $GrzB^+$ cells (Fig. 4H) were present in the $CD8_{OIM}{}^{Hi}$ subgroup compared with the other subgroups. Even though the GrzB density was significantly higher in the $CD8_{OIM}{}^{Lo}/FOXP3_{TC}{}^{Hi}$ compared with the $CD8_{OIM}{}^{Lo}/FOXP3_{TC}{}^{Lo}$, the $GrzB_{TC}/CD8_{TC}$ ratio was not different, suggesting no difference in CD8 cytotoxicity (Fig. 4H).

Classification and Regression Tree Subgroups as a Prognostic Marker in Multivariable Cox Regression

A multivariable Cox regression was performed to correct for MSI status, EBV status, T stage, N stage, Lauren classification, and type of surgery. The CART model remained an independent predictor of CSS, with HRs of 5.02 (95% CI: 2.03–12.42) for $CD8_{OIM}{}^{Lo}/FOXP3_{TC}{}^{Hi}$ and 7.99 (95% CI: 3.22-19.86) for $CD8_{OIM}{}^{Lo}/FOXP3_{TC}{}^{Lo}$, with $CD8_{OIM}{}^{Hi}$ as reference (Table 2).

Discussion

This study showed that $CD8_{OIM}$ cell density was the strongest prognostic marker in patients with GC, followed by the $FOXP3_{TC}$

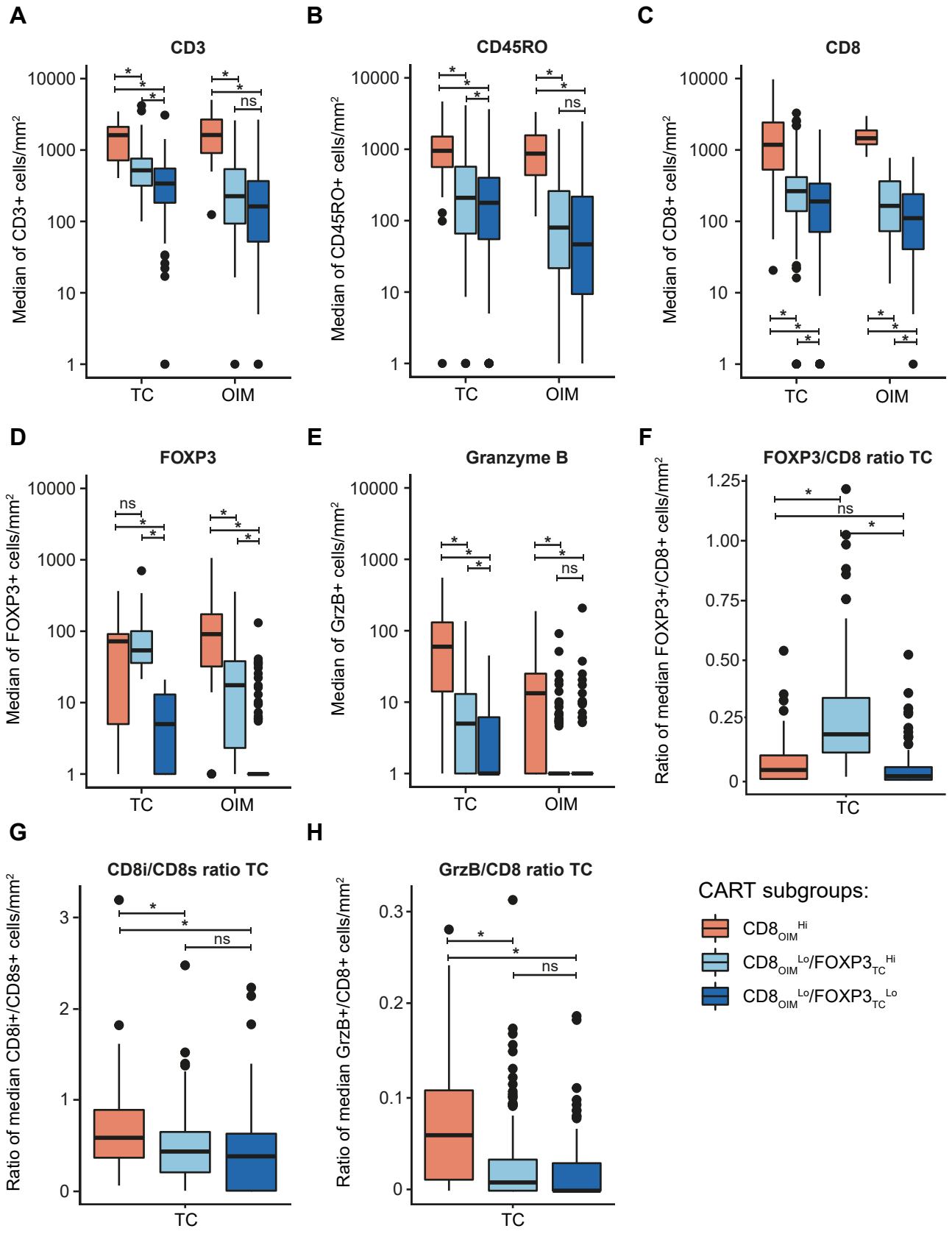

Figure 4.

Immune cell densities and ratios in the classification and regression tree (CART) subgroups. The median cell density (cells/mm^2) in log10 scale of (A) CD3, (B) CD45RO, (C) CD8, (D) FOXP3, and (E) granzyme B (GrzB) within the tumor center (TC) or outer invasive margin (OIM) of the 3 CART subgroups. (F) The ratio of FOXP3 divided by CD8 median cell densities in the TC. (G) The intraepithelial CD8 (CD8i) ratio is divided by stromal CD8 (CD8s) median cell densities in the TC. (H) The ratio of GrzB divided by CD8 median cell

Table 2
Multivariate Cox regression

Variable	HR (95% CI)	*P* value
CART model		
$CD8_{OIM}^{Hi}$	1.00 (reference)	
$CD8O_{IM}^{Lo}/FOXP3_{TC}^{Hi}$	5.02 (2.03–12.42)	<.0001
$CD8O_{IM}^{Lo}/FOXP3_{TC}^{Lo}$	7.99 (3.22–19.86)	<.0001
MSI status		
MSS	1.00 (reference)	
MSI-high	1.29 (0.72–2.31)	.385
EBV status		
EBV^{-}	1.00 (reference)	
EBV^{+}	2.06 (0.93–4.56)	.074
Lauren subtype		
Intestinal	1.00 (reference)	
Diffuse	1.15 (0.77–1.72)	.492
Mixed	1.4 (0.80–2.46)	.242
Other	1.11 (0.63–1.95)	.727
pT and pN stage (TNM eighth edition)		
pT1/2	1.00 (reference)	
pT3/4	3.46 (2.04–5.86)	<.0001
pN0	1.00 (reference)	
pN1–3	2.1 (1.33–3.31)	<.001
Surgery arm		
D1	1.00 (reference)	
D2	0.67 (0.48–0.95)	.025

Likelihood ratio test of the Cox model $P \leq$ 2e-16.
CART, classification and regression tree; EBV, Epstein-Barr virus; MSI, microsatellite instable; MSS, microsatellite stable; pT stage, pathological T-stage; pN stage, pathological N-stage; TNM, Tumor Regional Lymph Node and Metastasis Classification of Malignant Tumors according to the eighth edition.

density. The biomarker combination generated 3 immune subgroups, $CD8_{OIM}^{Hi}$, $CD8_{OIM}^{Lo}/FOXP3_{TC}^{Hi}$, and $CD8_{OIM}^{Lo}/FOXP3_{TC}^{Lo}$, and was an independent predictor of CSS in this cohort of patients treated with surgery only. Moreover, because these tumors were treatment-naive, these subgroups may also reflect the biology of the tumor.

In multiple studies of GC, the CD8 density was identified as a prognostic marker in the IM alone[13,16,27] or in both the TC and IM.[17,18] Our results showed that the CD8 in the OIM outperformed CD8 in the TC as a prognostic marker. This may explain why some of the studies that included the TC alone did not recognize the significance of the prognostic value of CD8.[14,28] The prognostic value of CD8 in the IM was also recognized for colorectal cancer by Galon et al,[29] where CD8 and CD3 in the IM were incorporated into their Immunoscore, together with the densities in the TC. The tumors with high $CD8_{OIM}$ density generally harbored high CD8 densities in the TC, resembling what is often called a "hot" immune phenotype with improved outcomes.[30]

Consistent with the results from 2 previous studies,[31,32] EBV^{+} and MSI-high tumors in our study displayed higher T-cell densities and were enriched in the $CD8_{OIM}^{Hi}$ "hot" immune subgroup. Even though EBV^{+} and MSI tumors are considered subgroups with superior prognoses,[22] in a multivariable analysis with correction for the 3 immune subgroups, we identified that they were not independent predictors of CSS. This is in line with Challoner et al,[14] who included FOXP3 and CD45RO in their stomach cancer immune score. In both ours and the study by Challoner et al,[14] MSI-high and EBV^{+} tumors showed heterogeneity of T-cell densities and were present in all immune subgroups. The heterogeneity in T-cell density in MSI-high tumors was also noted in colorectal MSI tumors,[33,34] and may be explained by the variable expression of immunogenic neoantigens[33] and immune evasion pathways.[34] In addition, survival analysis of the 3 immune subgroups within the GS and CIN subgroups separately showed a similar association with survival as for the whole series, indicating that the superior survival of the $CD8_{OIM}^{Hi}$ "hot" immune subgroup was not caused just by the EBV^{+} and MSI-high cases. This supports our finding that the immune phenotype provides additional information complementary to the TCGA molecular subgroups with added prognostic significance.

The role of $FOXP3^{+}$ Tregs in antitumor immunity is controversial, as it is associated with a worse patient outcome in most cancer types.[35] Our study showed a clear association of high $FOXP3^{+}$ cell density in the TC with improved survival, consistent with a previous large study in treatment-naive resectable GC.[14] It is not clear why higher densities of $FOXP3_{TC}$ correlated to improved prognosis in the $CD8_{OM}^{Lo}$ subset. One explanation is that $FOXP3^{+}$ Treg infiltration in the tumor reflects the initially activated immune state of the tumor, followed by immune escape strategies involving $FOXP3^{+}$ Tregs.[36] The presence of this preexisting immune response is more favorable for prognosis than an "immune cold" phenotype.[37] Alternatively, $FOXP3^{+}$ Tregs can have multiple phenotypes, including nonsuppressive, as revealed in a single-cell RNA sequencing study in GC.[38] Thus, a better understanding of the heterogeneity and functions of $FOXP3^{+}$ T cells may identify novel therapeutic targets of the tumor immune microenvironment in GC.

The added prognostic value of the OIM may be explained by the biological characteristics of the IM. The IM is an interface with interactions of pro- and antitumoral factors,[39] where the activated immune cells act as border security to prevent cancer dissemination. This is supported by findings in colorectal cancer (CRC); the Immunoscore in CRC was shown to correlate with a lower risk of recurrence.[40,41] Furthermore, a high T-cell infiltration and cytotoxic activity in the TC and IM was correlated with an absence of early histologic signs of metastatic invasion (venous emboli, lymphatic, and perineural invasion).[15,42] Moreover, the distant metastasis of CRC was associated with a lower Immunoscore,[29] reduced cytotoxicity in the TC, and reduced lymphatic vessel density at the IM.[42] Because patients in the $CD8_{OIM}^{Hi}$ subgroup had a long CSS, conceivably also in GC, the IM may be involved in preventing disease recurrence. These findings underline the importance of measuring the immune microenvironment in the IM.

We showed that higher T-cell densities in the TC and OIM were also associated with decreased lymph node status measured as the N stage. The association between immune cell density and lymph node metastasis has previously been shown in GC.[43] Therefore, T-cell density has potential value in predicting which patients are at risk of developing lymph node metastasis. This may be specifically relevant in patients with T1 stage GC (early GC) for whom advanced endoscopic resection is indicated rather than gastrectomy.[44] Some of these patients develop lymph node metastasis after endoscopic resection and still require subsequent gastrectomy. Because advanced endoscopic resections contain both TC and IM, T-cell densities can be reliably determined for endoscopic resection specimens. T-cell densities may contribute to risk assessment for the development of lymph node metastasis, which may potentially change treatment or surveillance strategies.[45] This information may also be of value prior to the endoscopic resection because high-risk patients may benefit from immediate gastrectomy.[46] However, to this end, T-cell density

densities in the TC. The boxplots depict the median density and IQR (25% to 75%). The pairwise Wilcoxon rank sum test was used to calculate *P* values. To depict the densities on the log10 y-axis, density was offset by 1. Statistics were performed before log transformation.

should be assessed in the diagnostic biopsy, which lacks information on the IM.

Information on T-cell densities as assessed on diagnostic biopsies would be essential in clinical practice, but only when it proves to be of predictive value for response to treatment. In the current Western guideline for resectable GC, perioperative chemotherapy is recommended, and the prognostic immune subgroups do not affect treatment decisions.[47] However, T-cell density may also predict the response to adjuvant chemotherapy, as shown in surgical resections by Jiang et al.[48] Target therapy options are being explored, such as anti-PD1[49,50] and other emerging markers[51] for which strong predictive biomarkers are needed. If such treatment is given before surgery, a biopsy is the only tissue that can be used to assess T-cell densities. However, the challenges of biopsies are the frequent lack of invasive margins and limited representation of the intratumoral heterogeneity due to its small size. With this in mind, it will be important to analyze how well the tumor immune biology is reflected in actual diagnostic biopsy specimens. Furthermore, whether T-cell densities have predictive value for response to specific treatment options requires further studies.

An important limitation of this study was the lack of a validation cohort to evaluate the cut-off values of CD8 and FOXP3 T-cell densities. Nonetheless, the cut-off values were useful in identifying clinically relevant subgroups that can be further explored for clinical implementation. Because of the large sample size and the performance of the CART analysis with 5-fold cross-validation, we assume that the cut-off values are reliable in this study; however, independent validation is preferred.

In conclusion, the clinical implication of this study is that the combination of $CD8_{OIM}$ and $FOXP3_{TC}$ is a strong and independent predictor of survival. Our results underscore that both the density and location of immune cells are highly relevant in GC. Independent validation of the identified subgroups is warranted, as well as evaluation of the predictive value to treatment regimens when chemo(radio)therapy or immunotherapy is added to surgery.

Acknowledgments

The authors thank the Dutch National Tissuebank Portal for facilitating the collection of archival tumor formalin-fixed and paraffin-embedded samples from patients with GC who participated in the Dutch D1/D2 trial.

Author Contributions

Conceptualization: T.S., N.v.G., B.Y., and H.v.L.; Methodology: T.S., N.v.G., B.Y., H.v.L., A.M., Y.K., and E.v.D.; Formal analysis: T.S. and H.B.; Investigation: T.S., H.B., J.E., and N.v.G.; Resources (patients): H.H. and C.v.d.V.; Data curation: N.v.G. and E.M.; Visualization: T.S.; Funding acquisition: N.v.G., H.v.L., and B.Y.; Project administration: N.v.G.; Supervision: N.v.G., B.Y., and H.v.L.; Writing – original draft: T.S.; Writing – review and editing: all authors. All authors read and approved the final version of the manuscript.

Data Availability

Anonymized data are available from the corresponding author upon reasonable request.

Funding

This work was supported by the Dutch Cancer Society (grant number KWF10613).

Declaration of Competing Interest

The authors declare no conflicts of interest.

Ethics Approval and Consent to Participate

This study was performed in accordance with the Declaration of Helsinki. The D1/D2 trial was approved by the medical ethical committee of the Leiden University Medical Center. The Dutch Code of Conduct for Responsible Use of Human Tissue allows for the analysis of residual tissue specimens obtained for diagnostic purposes and anonymized publication of the study results.

Supplementary Material

The online version contains supplementary material available at https://doi.org/10.1016/j.modpat.2023.100218

References

1. Bray F, Ferlay J, Soerjomataram I, Siegel RL, Torre LA, Jemal A. Global cancer statistics 2018: GLOBOCAN estimates of incidence and mortality worldwide for 36 cancers in 185 countries. *CA Cancer J Clin*. 2018;68(6):394–424.
2. Al-Batran SE, Homann N, Pauligk C, et al. Perioperative chemotherapy with fluorouracil plus leucovorin, oxaliplatin, and docetaxel versus fluorouracil or capecitabine plus cisplatin and epirubicin for locally advanced, resectable gastric or gastro-oesophageal junction adenocarcinoma (FLOT4): a randomised, phase 2/3 trial. *Lancet*. 2019;393(10184):1948–1957.
3. Gullo I, Carneiro F, Oliveira C, Almeida GM. Heterogeneity in Gastric Cancer: From Pure Morphology to Molecular Classifications. *Pathobiology*. 2018;85(1-2):50–63.
4. Bass AJ, Thorsson V, Shmulevich I, et al. Comprehensive molecular characterization of gastric adenocarcinoma. *Nature*. 2014;513(7517):202–209.
5. Berlth F, Bollschweiler E, Drebber U, Hoelscher AH, Moenig S. Pathohistological classification systems in gastric cancer: diagnostic relevance and prognostic value. *World J Gastroenterol*. 2014;20(19):5679–5684.
6. Ho SWT, Tan P. Dissection of gastric cancer heterogeneity for precision oncology. *Cancer Sci*. 2019;110(11):3405–3414.
7. Chen DS, Mellman I. Oncology meets immunology: the cancer-immunity cycle. *Immunity*. 2013;39(1):1–10.
8. Dunn GP, Bruce AT, Ikeda H, Old LJ, Schreiber RD. Cancer immunoediting: from immunosurveillance to tumor escape. *Nat Immunol*. 2002;3(11):991–998.
9. Zou W. Regulatory T cells, tumour immunity and immunotherapy. *Nat Rev Immunol*. 2006;6(4):295–307.
10. Lee JS, Won HS, Sun S, Hong JH, Ko YH. Prognostic role of tumor-infiltrating lymphocytes in gastric cancer: A systematic review and meta-analysis. *Medicine (Baltimore)*. 2018;97(32):e11769.
11. Yu PC, Long D, Liao CC, Zhang S. Association between density of tumor-infiltrating lymphocytes and prognoses of patients with gastric cancer. *Medicine (Baltimore)*. 2018;97(27):e11387.
12. Jiang W, Liu K, Guo Q, et al. Tumor-infiltrating immune cells and prognosis in gastric cancer: a systematic review and meta-analysis. *Oncotarget*. 2017;8(37):62312–62329.
13. Jiang Y, Zhang Q, Hu Y, et al. ImmunoScore Signature: A Prognostic and Predictive Tool in Gastric Cancer. *Ann Surg*. 2018;267(3):504–513.
14. Challoner BR, von Loga K, Woolston A, et al. Computational Image Analysis of T-Cell Infiltrates in Resectable Gastric Cancer: Association with Survival and Molecular Subtypes. *J Natl Cancer Inst*. 2020;113(1):88–98.
15. Pagès F, Berger A, Camus M, et al. Effector memory T cells, early metastasis, and survival in colorectal cancer. *N Engl J Med*. 2005;353(25):2654–2666.
16. Uppal A, Dehal A, Chang S-C, et al. The Immune Microenvironment Impacts Survival in Western Patients with Gastric Adenocarcinoma. *J Gastrointest Surg*. 2020;24(1):28–38.
17. Yun S, Koh J, Nam SK, et al. Immunoscore is a strong predictor of survival in the prognosis of stage II/III gastric cancer patients following 5-FU-based adjuvant chemotherapy. *Cancer Immunol Immunother*. 2021;70(2):431–441.
18. Kemi N, Hiltunen N, Väyrynen JP, et al. Immune Cell Infiltrate and Prognosis in Gastric Cancer. *Cancers (Basel)*. 2020;12(12).
19. Wang M, Huang YK, Kong JC, et al. High-dimensional analyses reveal a distinct role of T-cell subsets in the immune microenvironment of gastric cancer. *Clin Transl Immunology*. 2020;9(5):e1127.
20. Songun I, Putter H, Kranenbarg EM, Sasako M, van de Velde CJ. Surgical treatment of gastric cancer: 15-year follow-up results of the randomised nationwide Dutch D1D2 trial. *Lancet Oncol*. 2010;11(5):439–449.

21. Brierley JD, Gospodarowicz MK, Wittekind C. *The TNM classification of malignant tumours*. 8th ed. John Wiley & Sons; 2017.
22. Biesma HD, Soeratram TTD, Sikorska K, et al. Response to neoadjuvant chemotherapy and survival in molecular subtypes of resectable gastric cancer: a post hoc analysis of the D1/D2 and CRITICS trials. *Gastric Cancer*. 2022;25(3):640–651.
23. Laurén P. The two histological main types of gastric carcinoma: diffuse and so-called intestinal-type carcinoma. *Acta Pathol Microbiol Scand*. 1965;64(1):31–49.
24. COREON. Gedragscode Gezondheidsonderzoek. Commissie Regelgeving Onderzoek. www.coreon.org/gedragscode-gezondheidsonderzoek/
25. Bankhead P, Loughrey MB, Fernández JA, et al. QuPath: Open source software for digital pathology image analysis. *Sci Rep*. 2017;7(1):16878.
26. Junttila A, Helminen O, Väyrynen JP, et al. Immunophenotype based on inflammatory cells, PD-1/PD-L1 signalling pathway and M2 macrophages predicts survival in gastric cancer. *Br J Cancer*. 2020;123(11):1625–1632.
27. Heo YJ, Lee T, Byeon S-J, et al. Digital image analysis in pathologist-selected regions of interest predicts survival more accurately than whole-slide analysis: a direct comparison study in 153 gastric carcinomas. *J Pathol Clin Res*. 2021;7(1):42–51.
28. Pötzsch M, Berg E, Hummel M, et al. Better prognosis of gastric cancer patients with high levels of tumor infiltrating lymphocytes is counteracted by PD-1 expression. *Oncoimmunology*. 2020;9(1):1824632-1824632.
29. Galon J, Costes A, Sanchez-Cabo F, et al. Type, density, and location of immune cells within human colorectal tumors predict clinical outcome. *Science*. 2006;313(5795):1960–1964.
30. Chen DS, Mellman I. Elements of cancer immunity and the cancer–immune set point. *Nature*. 2017;541(7637):321–330.
31. Chiaravalli AM, Feltri M, Bertolini V, et al. Intratumour T cells, their activation status and survival in gastric carcinomas characterised for microsatellite instability and Epstein-Barr virus infection. *Virchows Arch*. 2006;448(3):344–353.
32. Cho J, Chang YH, Heo YJ, et al. Four distinct immune microenvironment subtypes in gastric adenocarcinoma with special reference to microsatellite instability. *ESMO Open*. 2018;3(3):e000326-e000326.
33. Mlecnik B, Bindea G, Angell HK, et al. Integrative Analyses of Colorectal Cancer Show Immunoscore Is a Stronger Predictor of Patient Survival Than Microsatellite Instability. *Immunity*. 2016;44(3):698–711.
34. Kim JH, Seo M-K, Lee JA, et al. Genomic and transcriptomic characterization of heterogeneous immune subgroups of microsatellite instability-high colorectal cancers. *J Immunother Cancer*. 2021;9(12):e003414.
35. Shang B, Liu Y, Jiang S-j, Liu Y. Prognostic value of tumor-infiltrating FoxP3+ regulatory T cells in cancers: a systematic review and meta-analysis. *Sci Rep*. 2015;5(1):15179.
36. Fridman WH, Zitvogel L, Sautès–Fridman C, Kroemer G. The immune contexture in cancer prognosis and treatment. *Nat Rev Clin Oncol*. 2017;14(12):717–734.
37. Ward-Hartstonge KA, McCall JL, McCulloch TR, et al. Inclusion of BLIMP-1+ effector regulatory T cells improves the Immunoscore in a cohort of New Zealand colorectal cancer patients: a pilot study. *Cancer Immunol Immunother*. 2017;66(4):515–522.
38. Sathe A, Grimes SM, Lau BT, et al. Single-Cell Genomic Characterization Reveals the Cellular Reprogramming of the Gastric Tumor Microenvironment. *Clin Cancer Res*. 2020;26(11):2640–2653.
39. Zlobec I, Lugli A. Invasive front of colorectal cancer: dynamic interface of pro-/anti-tumor factors. *World J Gastroenterol*. 2009;15(47):5898–5906.
40. Bindea G, Mlecnik B, Galon J. Tumor spread or siege immunity: dissemination to distant metastasis or not. *Oncoimmunology*. 2021;10(1):1919377.
41. Pagès F, Mlecnik B, Marliot F, et al. International validation of the consensus Immunoscore for the classification of colon cancer: a prognostic and accuracy study. *Lancet*. 2018;391(10135):2128–2139.
42. Mlecnik B, Bindea G, Kirilovsky A, et al. The tumor microenvironment and Immunoscore are critical determinants of dissemination to distant metastasis. *Sci Transl Med*. 2016;8(327):327ra26.
43. Lee HE, Chae SW, Lee YJ, et al. Prognostic implications of type and density of tumour-infiltrating lymphocytes in gastric cancer. *Br J Cancer*. 2008;99(10):1704–1711.
44. Sekiguchi M, Oda I, Taniguchi H, et al. Risk stratification and predictive risk-scoring model for lymph node metastasis in early gastric cancer. *J Gastroenterol*. 2016;51(10):961–970.
45. Wei J, Zhang Y, Liu Y, et al. Construction and Validation of a Risk-Scoring Model that Preoperatively Predicts Lymph Node Metastasis in Early Gastric Cancer Patients. *Ann Surg Oncol*. 2021;28(11):6665–6672.
46. Liu Q, Ding L, Qiu X, Meng F. Updated evaluation of endoscopic submucosal dissection versus surgery for early gastric cancer: A systematic review and meta-analysis. *Int J Surg*. 2020;73:28–41.
47. Lavacchi D, Fancelli S, Buttitta E, et al. Perioperative Tailored Treatments for Gastric Cancer: Times Are Changing. *Int J Mol Sci*. 2023;24(5).
48. Jiang Y, Xie J, Huang W, et al. Tumor Immune Microenvironment and Chemosensitivity Signature for Predicting Response to Chemotherapy in Gastric Cancer. *Cancer Immunol Res*. 2019;7(12):2065–2073.
49. Janjigian YY, Van Cutsem E, Muro K, et al. MATTERHORN: phase III study of durvalumab plus FLOT chemotherapy in resectable gastric/gastroesophageal junction cancer. *Future Oncol*. 2022;18(20):2465–2473.
50. Bang YJ, Van Cutsem E, Fuchs CS, et al. KEYNOTE-585: Phase III study of perioperative chemotherapy with or without pembrolizumab for gastric cancer. *Future Oncol*. 2019;15(9):943–952.
51. Röcken C. Predictive biomarkers in gastric cancer. *J Cancer Res Clin Oncol*. 2023;149(1):467–481.